Transactions of the Nigerian Association of Mathematical Physics
Volume 3, (January, 2017), **pp 177 – 188**
© Trans. of NAMP

The Convergence of No-Reference and Full-Reference in Objective Image Quality Assessment

Vincent O.R., Makinde S.A. and Ojo O.E.

Department of Computer Science, Federal University of Agriculture, Abeokuta, Ogun State, Nigeria.

Abstract

The diversities of no-reference and full-reference objective image quality assessments are expressed in their presentation and focus. Uncontrolled variation is a major challenge associated with the accessibility and non-availability of reference images. In this paper, the convergence of two objective image quality assessments, power spectral and structural similarity image metric (SSIM), which are examples of a no-reference and full-reference objective image quality assessments, respectively have been investigated. We analyzed the diverse focus of the two models and examined the sharpness and contrast. Power spectrum was analyzed by varying the illumination constant c from 1 to 5 while SSIM was applied to each variation in order to actualize the frequency. The result shows that contrast illumination remains the convergent point of the two models and their combination proves a better alternative for effective image quality assessment.

Keywords: Objective Image Quality Assessment, MSE, PSNR, SSIM and Power Spectra

1.0 Introduction

Image quality plays an important role in various applications and the primary goal is to supply the quality metrics that can predict perceived image quality automatically. Assessing quality level in image is important for image computing and video processing applications[1, 2].Image quality assessment would continue to be a focus of research for several reasons. Assessing quality is important for scientific visualization, gaming and movie industries, medical imaging, mobile video; and more importantly for computer aided designs[3].Digital images are exposed to a numerous varieties of alterations which occur during acquisition, processing, compression, storage, transmission and reproduction[4, 5]. Images are obtained by camera devices that may introduce distortions due to sensor noise, color calibration, exposure control, camera motion etc. [6]. Images may further go through many stages of processing before being presented to human observer and each stage of processing may introduce distortions that could affect the quality of the final display. Compression techniques, which reduce bandwidth requirements for storage and transmission, also allow certain signal distortions [7].

Images are usually affected by some basic nuisances expressed in illumination variations and distance from camera; pose invariance, time delay, occlusions and facial corruption or disguise like makeup, beard, and glasses [8-11]. A degradation of image quality also occurs during quantization process of lossy compression technique. Similarly, bit errors which occur during image transmission over a channel or when it is stored, also tend to introduce distortions.

Other major challenges are unconstraint illumination and pose invariance quality assessment [12-16]. In situations where little information are given about the source target, illumination transfer could pose more challenges [17, 18]. It affects the appearance of an object in numerous ways, and the resulting variation in appearance constitute a major source of difficulty for designing many image-based applications [19]. Generally, humans represent images under radically different illumination conditions. However, recognition of images is sensitive to illumination direction [20]. Research has shown that the most common image representations such as edge maps or Gabor-filtered images are not capable of overcoming illumination changes [21-23]. Quality assessment metric is therefore important in order to determine the level of distortions[24, 25].

Corresponding author: Vincent O.R., E-mail: vincent.rebecca@gmail.com, Tel.: +2347037832842

Several techniques have been proposed for image quality assessment. Many of these techniques were based on either objective no-reference, full reference or reduce reference[26, 27]. Studies on no-reference include image assessment by training General Regression Neural Network (GRNN) to access a range of distortion types, Logarithmic Total Variation (LTV) by transferring illumination from a source image to a target image, assessment of visual quality of Depth-Image-Based Rendering (DIBR) related distortions, algorithms for JPEG compression of images and power spectra [2, 17, 28, 29]. Reduced-reference (RR) possesses some information regarding the reference image, for example, in watermark, which are not actual reference image itself, apart from the distorted image. A wavelet packet analysis for rotation and scale invariant is an example of this assessment [30, 31].

Full-reference has been used in diverse ways for assessment. Some full reference models include Practical Image Quality Index, NPID (Normalized Perceptual Information Distance), MS-SSIM (Multi Scale Structural Similarity Index Measure), Content Partitioned Structural Similarity Index, FSIM (Feature Based Structural Similarity Index), MAD (Most Apparent Distortion), and SSIM (Structural Similarity Index Measure) [32-37]. SSIM and power spectra remain the most popular of the FR and NR, respectively; but no studies have examined and analyzed their common point. However, comparison have been made between the two well-known objective IQA models, the peak-signal-to-noise ratio (PSNR) and structural similarity index measure (SSIM) [38].

Motivated by the foregoing, we examined, compared and analyzed in this paper, the meeting point between power spectrum and SSIM in accessing image quality and argue that though they are no-reference and full-reference objective IQA models respectively. We also argued that a convergent point exist between the two objective image assessment techniques. Analysing and understanding image inputsacross their various length-scales of variation provides a natural framework for the analysis of data with spatial coherence because the spectral in itself provides an appropriate domain for parameter optimization, as the frequency basis captures typical filter structure well [39].We examine the sharpness, tone reproduction and contrast. Power spectrum was analyzed by varying the illumination constant *c* from 1 to 5 while SSIM was applied to each variation in order to actualize the frequency effect on the variations. Illumination measurement was perceived to be an optimization of the efficiency of power spectrum.

2.0 Image Quality Assessment(IQA) Models

The two main image quality assessment models are the subjective and the objective IQA. The **s**ubjective assessment offersprecise and authentic way of assessing visual qualitywhen dealing with bulky number of subjects. An obvious problem that arises is that assessment criterion may vary from person to person. In subjective quality measure, the distorted image quality is specified by the Mean Opinion Score (MOS) which is the result of perception based on subjective evaluation.The MOS is generated by averaging the result of a set of standard subjective tests and it serves as an indicator of the perceived image quality[40, 41]. Nevertheless,literature has revealed that subjective assessment is costly, cumbersome, and inappropriate for in-service and real-time applications[42-44].Furthermore, the environment and the mood of the subjects usually affect the subject assessment which may lead to reduced consistent results especially in situations where by the subject pool is not big enough[45]. Objective IQA was introduced to address these because it has far-flung applicationsandtherefore attracts attention of researchers.

Objective quality assessment is represented withmathematical algorithms and models for image quality assessment that could analyze images and report their quality without human involvement[28]. These methods could eliminate the need for expensive subjective studies [6, 36, 46]. The objective quality measure plays variety of roles which include monitoring and controlling of image quality for quality control systems; benchmarking image processing systems; optimization of algorithms and parameters; better management of digital photos and evaluation ofphotographing skills by home users.Objective image quality measure could be classified according to the availability of the reference image, that is, reference or distortion-free image with which distorted image is to be compared[47]. These classifications are into three categories, full-reference (FR), no- reference (NR) and reduced- reference (RR)[48].

In full-reference,the reference image is assumed to be known with its inputimage compared with the distorted one. The quality of the distorted image is accessed by the reference image[49]. The most widely used full- reference image quality metrics are the mean square error (MSE) and peak to signal noise ratio (PSNR). MSE involves computing an error signal by subtracting the test signal from the reference, and then computing the average energy of the error signal. This metric has been frequently used in signal processing and is defined as

$$\mathrm{MSE} = \frac{1}{\mathrm{MN}} \sum_{\mathrm{i}=1}^{\mathrm{M}} \sum_{\mathrm{j}=1}^{\mathrm{N}} (\mathrm{x(i,j)} - \mathrm{y(i,j)})^2 , \quad (1)$$

Where *x(i, j)* represents the reference image and *y(i, j)* represents the distorted image;*M* and *N* are the width and height[50]. On the other hand, PSNRis inversely proportional to the MSE and it is evaluated in decibels, defined as

$$\mathrm{PSNR} = 10 \log_{10} \frac{\mathrm{L}^2}{\sqrt{\mathrm{MSE}}}, \quad (2)$$

where*L* is the dynamic range of the pixel values. It is assumed that higher PSNR value corresponds to a higher image quality and vice versa. The Structural Similarity Index Metrics (SSIM) is a full-reference image quality assessment metric which has

shown promising of better quality assessment than the inappropriate MSE and PSNR with reasonable computational complexity increase [43, 51-53].

However, no-reference, for example energy spectrum is a divergent to SSIM, having access only to the distorted image signal and the quality of the signal is being assessed without any knowledge of the reference image. The algorithms detect specific types of distortion such as blurring, blocking, ringing, or various forms of noise [54]. It is a quality assessment of an image using an algorithm such that the only information that the algorithm receives and makes a prediction on quality is the distorted image whose quality is being assessed [29].In many practical applications where the reference image is not available, a no-reference quality assessment approach is desirable.Reduced-referencequality assessment algorithm uses the partial reference image information to assess the quality of the distorted image[29]. The reference image is only partially available, in the form of a set of extracted features made available as side information to help the quality evaluation of the distorted image.

This study combines full-reference using SSIM and no-reference assessments, energy power spectrum in order to measure a convergent point of the divergent in assessments. Strength of the image variations and diverse variant quality were measured. The power spectral density (PSD) shows the strength of the variations as a function of frequency, while SSIM reveals its dimension of quality changes. The reference image was made available in SSIM and the distorted at different illuminations made accessible in power spectra.

3.0 No-Reference (NF) and Full Reference (FR) Divergence

No-reference (NF), for example, power spectradoes not require access to the original image/video but searches for artifacts with respect to the pixel domain of an image, utilizes information embedded in the bitstream of the related image/video format, or performs quality assessment as a hybrid of pixel-based and bitstream-based approaches[34, 55, 56]. NF is used in wireless communications and telecommunication systems to quantify service quality delivery to end uses. It is germane to real-time objective quality assessment where resources are limited such as frequency spectrum in wireless communications.

In contrast, full-reference allows entire original image to be available as a reference. Accordingly, FR methods are based on comparing distortedimage with the original one [57, 58].The application scope of the metric includes image compression and, watermarking, etc. Full reference could be based on mean squared error (MSE), structural similarity index (SSIM), multi-scale structural similarity index (MS-SSIM), visual information fidelity (VIF), most apparent distortion (MAD), feature similarity index (FSIM), Saliency Map Analysis, and structural similarity index(SSIM), etc.[43, 59, 60].A FR method like SSIM, displays this diversity by demonstrate strong dependencies and these dependencies carry useful information about the structure of a scene as opposed to no-reference and capable of measuring structural information changes which provides a good approximation of perceived image distortion examined in this paper. This paper examines and analyses the diversities of power spectra and SSIM by varying the illumination constant.

A. Power Spectra

Power spectrum is directly related to the autocorrelation of an image, which shows how closely related two points *l(fx, fy)* image are as a function of their distance and orientation. To reduce redundancy as a valuable preprocessing strategy, an adequate model for the power spectrum of natural images is needed[61]. Research has shown that power spectrum of natural images dependson the spatial frequency,$1/f^{\alpha}$, where $\alpha \sim 2$[22, 62-64]. The mean power spectra using polar coordinates is given by

$$E[|I\ (f,\theta)|^2] \cong\ A_s(\theta)/f^{\alpha_s\,(\theta)}. \quad (3)$$

The shape of the spectra is a function of its orientation. The function $A_s(\theta)$ is the amplitude scaling factor of each orientation and $\alpha_s\,(\theta)$ is the frequency exponent as a function of orientation. The image principal components (IPCs) decompose the image using

$$i(x,y) = \sum_{n=1}^{p} u_n IPC_n(x,y) \quad , \quad (4)$$

where $i(x,y)$ is the intensity distribution of the image along spatial variables *x* and *y*. $P \leq N^2$ is the total number of IPCs and $N^2 = 256^2$ is the number of pixels of the image. $IPC_n(x,y)$ is the eigenvectors of the covariance matrix $\tau = [\,E(i-m)(i-m)^{\tau}$ where i represents the pixels of the images rearranged in a column vector. E is the expectation operator, $m = E\,[i]$ and u_n representthe mean of images and the coefficient for describing the image $i(x,y)$ respectively[65]. Power spectrum is computed by taking the squared magnitude of its Discrete Fourier Transform (DFT) given as:

$$\Gamma\big(k_{x\,,}k_y\,\big) = \frac{1}{N^2}\big|I\big(k_x,k_y\big)\big|^2 \ , \quad (5)$$

where

$$\mathrm{I}\big(k_{x\,,}k_y\,\big) = \tfrac{1}{N^2}\textstyle\sum_{x=0}^{N-1}\sum_{y=0}^{N-1} i(x,y)\exp\left(-\frac{j2\pi}{N}(xk_x + yk_x)\right), \quad (6)$$

$f_x = k_x/N$ and $f_y = k_y/N$ are discrete spatial frequencies. The power spectrum $\Gamma\big(k_{x\,,}k_y\,\big)$, encodes the energy density for each spatial frequencies and orientations over the whole image. PCA applied to power spectra gives the main components

that take into account the structural variability between images. The power spectrum is normalized with respect to its variance for each spatial frequency

$$\acute{\Gamma}(k_x,k_y) = \Gamma(k_x,k_y)/std[\Gamma(k_x,k_y)] \quad (7)$$

and standard deviation

$$std[\Gamma(k_x,k_y)] = \sqrt{E\left[(\Gamma(k_x,k_y) - E\left[\Gamma(k_x,k_y)\right])^2\right]}. \quad (8)$$

This normalization compensates for shape difference $1/f^{\alpha}$ of the power spectrum [66]. The spectral principal components (SPCs) decompose the normalized power spectrum, resulting to

$$\grave{\Gamma}_s(k_x,k_y) = \sum_{n=1}^{p} u_n SPC_n(k_x,k_y) \quad . \quad (9)$$

The frequency spectrum f_s and the power spectral density (PSD) are given in equation (10) and (11) respectively.

$$f_s = [-(n/2) + 1{:}\,1{:}\, n/2]^* df \quad (10)$$

$$PSD = f_s 10^* \log 10(pxf/\max pxf) \quad (11)$$

B. Structural Similarity Index Measure (SSIM)

SSIM is introduced for assessing quality of JPEG compressed image.The system uses a PNG format image as reference image which was converted to a JPEG format, a lossy compression technique. The JPEG image format was used as the compressed image. The two images are used for calculating SSIM index. SSIM Index was calculated for compressed images with different compression ratio. PSNR of the compressed images wasalso calculated.The SSIM algorithm assesses three quantities between two non-negative image signals *x* and *y*: the luminance *l*(*x, y*), contrast *c*(*x, y*), and structure *s*(*x, y*). Figure 1 is a modification of SSIM model in [4, 43].Luminance is modeled as average pixel intensity, contrast by the variance between the reference and distorted image, and structure measured by the cross-correlation between the two images.In general, similarity measuresmust satisfy the following conditions:

Symmetry: *S(x, y) = S(y, x).* When quantifying the similarity between two signals, exchanging the order of the input signals should not affect the resulting measurement.

Boundedness: *S(x, y) ≤1*. An upper bound can serve as an indication of how close the two signals are to being perfectly identical. Other algorithms like signal-to noise ratio type of measurements are typically unbounded.

Unique maximum: *S(x, y)* = 1 if and only if *x = y*. The perfect score is achieved only when the signals being compared are identical. In other words, the similarity measure would quantify any variations that may exist between the input signals[4].

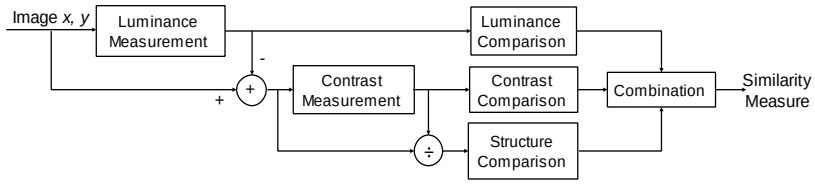

Figure 1: Structural Similarity Index Metric (Modified from [4] and [43]).

Let *x* represents the reference image sample, while *y* represent the lossy compressed image sample and there exist *NxM* array for simplicity. The system separates the task of similarity measurement into three components, which are luminance, contrast and structure as shown in figure 1.The first step is to measure the luminance of *x* and *y*, which is understood as the average luminance value of all pixels in an image and respectively indicated as μ_x and μ_y defined as

$$\mu_x = \frac{1}{N}\sum_{i=0}^{N-1} x_i \;\; ; \quad \mu_y = \frac{1}{N}\sum_{i=0}^{N-1} y_i \, . \quad (12)$$

That is, it is a measure of the ratio of summation of luminance values for each pixel in the image to the total number of pixels in the image (N). The function for the comparison of the luminance *l(x,y)* is defined as

$$l(x,y) = \frac{2\mu_x\mu_y + C_1}{\mu_x^2 + \mu_y^2 + C_1}. \quad (13)$$

In (13), $C_1$is given as $(K_1L)^2$, with K_1being an arbitrary constant $(<<1)$ usually set to *0.01* and *L* is equal to the maximum possible pixel value of the image. If 8bits per pixel is used, *L* invariably becomes 2^8*-1* which is *255*.The average contrast of each reference image *x* and compressed image *y* is determined by calculating the standard deviations of the two images respectively indicated using the expression:

$$\sigma_x = \left(\frac{1}{N-1}\sum_{i=0}^{N-1}(x_i - \mu_x)^2\right)^{1/2} ; \; \sigma_y = \left(\frac{1}{N-1}\sum_{i=0}^{N-1}(y_i - \mu_y)^2\right)^{1/2} \quad (14)$$

The contrast is compared by:

$$C(x,y) = \frac{\sigma_x\sigma_y + C_2}{\sigma_x^2 + \sigma_y^2 + C_2} \, , \quad (15)$$

C_2 is a constant usually equal to $(K_2L)^2$, with $K_2<<1$ and usually set to 0.03 [67]. The structure comparison function *s*(*x,y*) of the two image signals is calculated with

$$S(x,y) = \frac{\sigma_{xy} + C_3}{\sigma_x\sigma_y + C_3}, \quad (16)$$

$C_3 = C_2/2$, and the SSIM is therefore a combination of *x* and *y* properties of the images

$$\sigma_{xy} = \frac{1}{N-1}\sum_{i=0}^{N-1}(x_i - \mu_x)(y_i - \mu_y) \quad (17)$$

and it is gives as

$$SSIM(x,y) = \frac{(2\mu_x\mu_y + C_1)(2\sigma_{xy} + C_2)}{(\mu_x^2 + \mu_y^2 + C_1)(\sigma_x^2 + \sigma_y^2 + C_2)}. \quad (18)$$

C. The Convergence of Power Spectra and SSIM

Different illuminations of the same images are used in assessing the image quality. Figure 2 shows the proposed convergence model for power spectrum density (PSD) at different illuminations and SSIM. The PSD depicts the autocorrelation function transformation, and provided an interpretation of this transform. Figure 2 consists of four stages: the luminance comparison, pre-processing, processing and output stages. The stages are elucidated as follows:

Luminance Comparison: This stage simply starts the execution of the model by accepting two images as argument, with different illuminations. The difference in the illumination arises from the changes produced by the PSD transformation. The image database used to test our model is the well-known Lena image, which has been employed by many researchers in image processing.

Pre-processing: This stage typically performs a variety of basic operations by measuring the gradient of image. The reference and distorted images are set to align with each other for proper processing. In another perspective, noise is also eliminated. The quality assessment metrics convert the digital pixel values stored in luminance values of pixels through point-wise nonlinear transformations.

Processing: The salient features needed to compare the images are extracted with gradient measurement using the contrast sensitivity function (CSF). The CSF illustrates the sensitivity of the HVS to different spatial and temporal frequencies in the visual stimulus. Some of the image quality metrics are implemented using a linear filter which approximates the frequency response of the CSF. The contrast and structure of the images are later compared using structural similarity index (SSIM).

Output: The output is a measure of the similarity between the two images based on SSIM. This is based on the idea that the human visual system is highly adapted to process structural information and using the changes in the information between the reference and distorted image to give the final result[68].

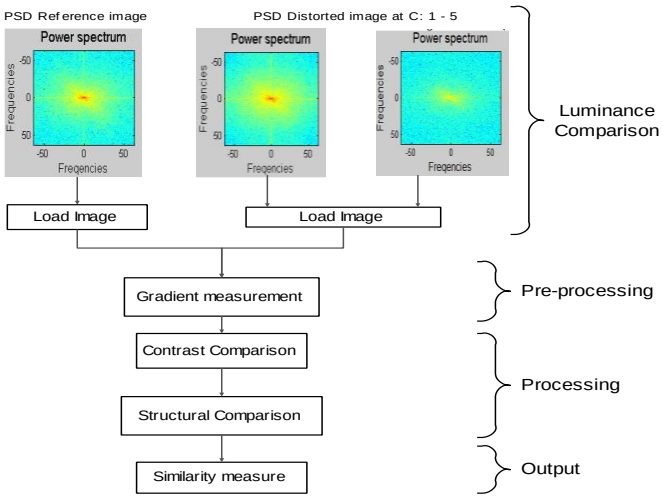

Figure 2: The Proposed Convergent Model for Power Spectra and SSIM

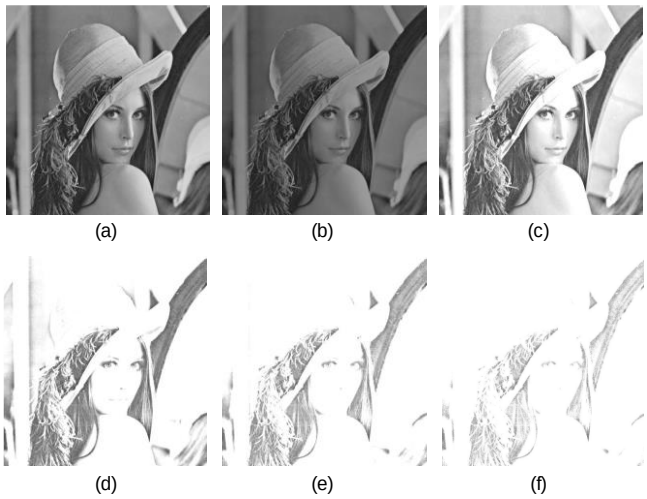

Figure 3: Illumination at different level of intensities. (a) is the original image; (b) is the illuminated image at constant, *c* =1; (c) is the illuminated at *c* =2; (d) is the illuminated *c* =3; (e) is the illuminated at *c* =3; and (f) is the illuminated at *c* =5.

4.0 Experimental Results

This section presents the detailed simulations, simulation environments and the simulated result of both schemes. Section 4.1, 4.2 and 4.3explained the simulation results of power spectrum, SSIM and their convergence respectively.

A. Power Spectrum

Illumination was done on the input image with principal component analysis (PCA) and power spectra used to measure the quality. This generated results for power and frequency spectra with equivalent power spectral density.

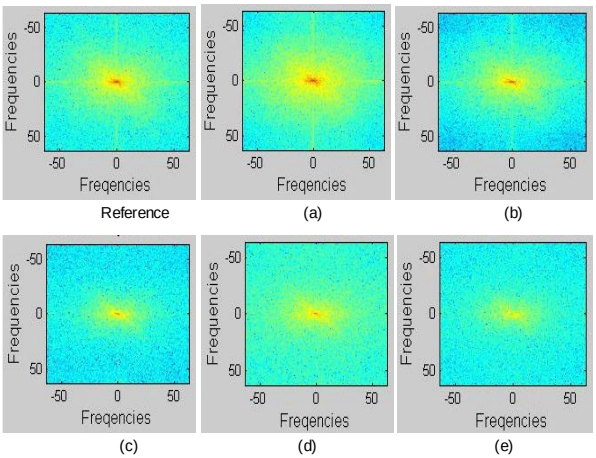

Figure 4: Power spectrum. Reference image, (a), (b), (c), (d), and are power spectra at c=1, 2, 3, 4, and 5 respectively.

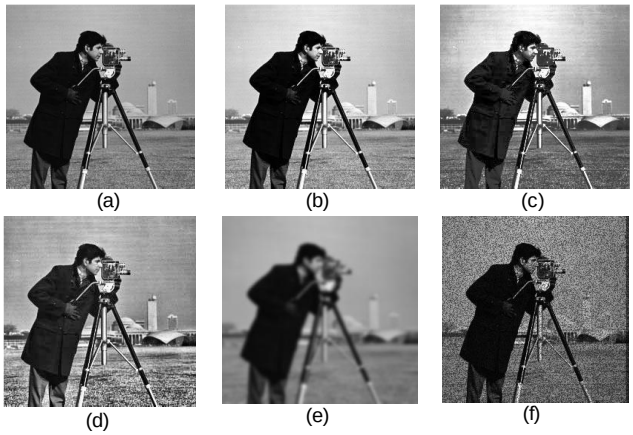

Figure 5: SSIM Diversity with Camera Image. Original image was extracted from [69] (a) Original with SSIM = 1, PSNR = INF, MSE = 0; (b) SSIM = 0.93, PSNR = 18.40, MSE = 947.48; (c) SSIM = 0.81, PSNR = 19.09, MSE = 808.08; (d) SSIM = 0.77, PSNR =20.59, MSE = 572.38;(e) SSIM = 0.72, PSNR = 22.42, MSE = 375.15; (f) SSIM = 0.42, PSNR = 15.76, MSE = 1741.52.

Figure 3 shows the power spectrum density image based on the illumination $c_i (i = 1, 2, \ldots 5)$. The result shows that the higher the value of *c*, the more the intensity of the image produced. Figure 4 shows the power spectrum results for each variation in figure 3.

Table 1: Image Diffusion Capacity

Lena Image (Kb)	Power Spectrum	Frequency Spectrum	Power Spectrum Density *(Hz)*e+15
82.7	Normal Spectrum	Normal	INF
27.1	Diffused	Rough	0.66
38.5	Very Diffused	Very Rough	2.5
34.6	More diffused	More Rough	3.6
27.1	Further Diffused	Further Rough	4.0
22.4	Further diffused than the previous image at 22kb	Further rough than the previous image	4.2

Table 1 presents the Lena image diffusion capacity at different compression levels. Table 1 shows the effects on the power spectra, frequency and PSD for varying image illumination constant. The simulated results in table 1 showed that the smaller the image size, the higher the PSD. The resulting PSD quality measure for each image 1, 2and 3 are 0.8, 0.6 and 0.5 *(Hz)*, which confirms that high quality depicts better PSD. Table 1 also shows that the more the image is further processed, the higher the power spectrum density and the power spectrum becomes more diffussed as the image size reduces.

In addition, the frequency spectrum becomes more rough when the image is further processed. In figure 4, an increase in the image intensity lowers the image size, leading to increase in power spectrum density. However, exception occurs when *c* is 1 where there exist a significant variation in the image size in figure 4 (a) and power spectrum density as compared with the trend when *c* is greater the 1. In terms of the power spectrum at c = 3, figures 3 shows more power compared to others.

B. SSIM

The first experiment was conducted using a single image with different compression ratio. The resolution of the reference image used was 716×550. Figure 5 shows the original image and the compressed images used for the experiment. The SSIM Index and PSNR for all the compressed images were calculated. Table 2 shows the SSIM and PSNR values for each of the compressed image samples. Asudden decrease in the value of PSNR was found after certain compression levels; whereas SSIM index indicates a better degradation of image quality. The sudden decrease in PSNR is because it is a measure of average error which is not consistent as the compression ratio increases. In Figure 5, a diversity of SSIM behavior with cameraman image is shown.

C. **The Convergence Results**

Figure 7 and 8 show the power spectrum density and the frequency spectrum for different bytes. The size of each variation was measure which in figure 9 compares the contrast of the images. In order to compare the image intensities with the original image, the four techniques were analyzed, namely, power spectra, SSIM, PSNR, and MSE. In MSE, when $x(i, j) = y$

(i, j), then the images differences tends to zero; implying that pixel-by-pixel matching of the images becomes perfect. However, if MSE is small enough, this corresponds to a high quality decompressed image. MSE therefore increases as the compression ratio increases.It is important to note that a value of 0 for MSE indicates perfect similarity which simply means that a value greater than one implies less similarity and will continue to grow as the average difference between pixel intensity increases. However, largerdifferences between pixel intensities do not necessarily indicates that the contents of the image are significantly different as shown in figure 10.

Table 2 shows the relationship the high range of power spectra could not be displayed in figure 10. Figure 10 reflects that as the image was further processed and the image size reduces, only MSE increases.To resolve some of the challenges of MSE for image comparison, PSNR was used which take the value derived from MSE in computing the final result. Also, it is important to note that the higher the PSNR the closer the distorted image is to the original. This simply indicates a higher PSNR value should correlate with a higher quality image. However, the experimental outcome does not always reflect the case.SSIM was used for image comparison and later used to compare with the other two image comparisons. At high level, SSIM tends to measure the change in luminance, contrast and structure in an image.

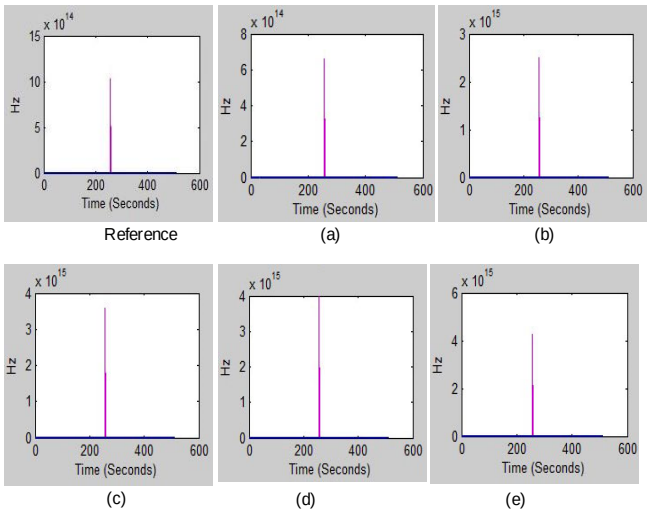

Figure 7: Power Spectrum Density of Lena Image for different image intensities (a)Reference with 82741 bytes; (b) 27065 bytes; (c) 38533 bytes (d) 34561 bytes (e) 27144 bytes; (f) 22351 bytes.

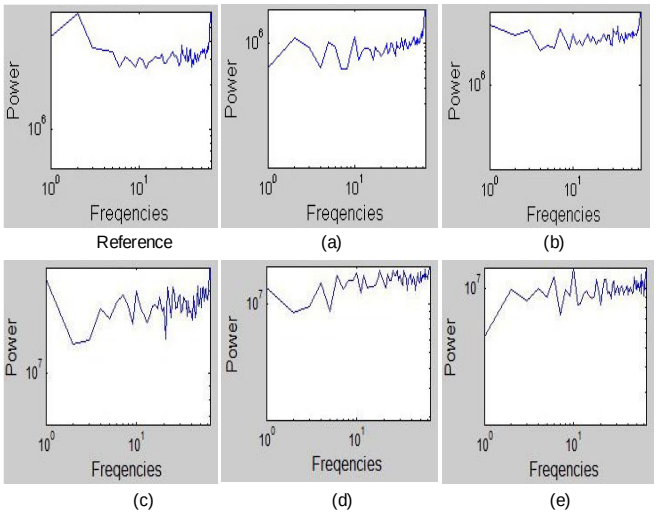

Figure 8: Frequency Spectrum of Lena Image. Reference is 82741 bytes; (a) Variation at c+1; 27065 bytes; (b) 38533 bytes (c) 34561 bytes (d) 27144 bytes; (e) 22351 bytes.

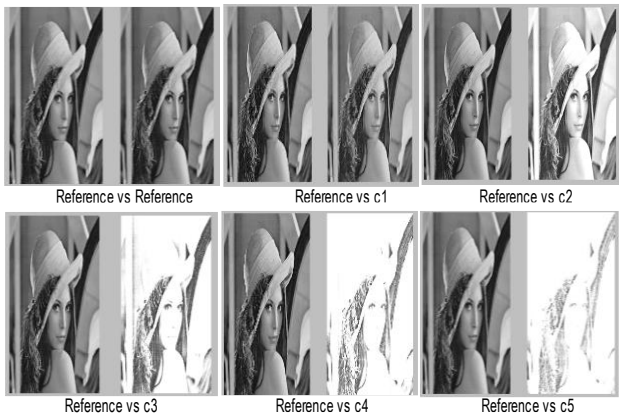

Figure 9: Image Intensity Comparisons. Reference image was extracted from [70]

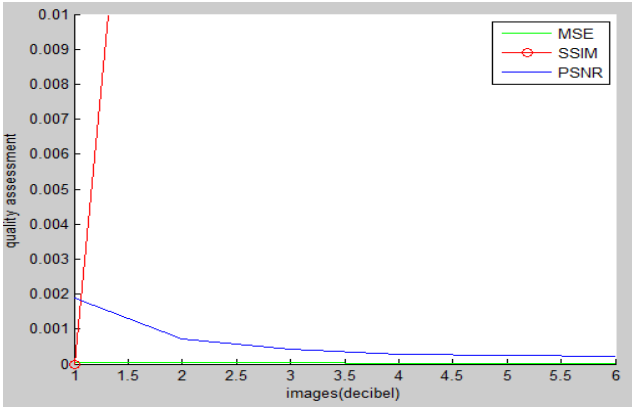

Figure 10: Quality Assessment using MSE, SSIM, and PSNR

Table 2: The Assessment of four Quality Measures

Image Size (Byte)	PSD	SSIM	PSNR	MSE
82741	1.0320e+15	1	INF	0
27065	6.5947e+14	0.89	18.90	18.90
38533	2.4959e+15	0.80	11.24	4930.98
34561	3.5928e+15	0.56	7.32	12147.09
27144	3.9984e+15	0.50	6.33	15272.21
22351	4.2453e+15	0.47	5.74	17492.48

The resulting power spectral density quality measure for figure 7a, b, c, d, e are 0.65, 2.50, 3.59, 4.00 and 4.24 e+15 *(Hz)*, which indicates that the better the quality of the image the higher and better its power spectral density.The frequency spectrum becomes rough as the quality of the image depreciated.The observation of the ring pattern in the power spectrum which indicates poor image quality and hence a more diffused power spectrum. As structural similarity index approaches1, the quality of the image is close to the original image**.**

5.0 Conclusion

In this paper, a meeting point for power spectrum and SSIM in image quality assessment was examined and analyzed. The results and analysis showed that SSIM is more efficient as it is more consistent with human eye observation. The boundedness property of Structural Similarity Index $(S(x,y) \leq 1)$, which serves as an indication of how close the two image signals are also enhance the effectiveness of SSIM in assessing image quality. Therefore, SSIM could be a useful toolfor better assessment and would be an effective alternate. Furthermore, SSIM simulated results indicated that MSE and PSNR are very simple, easy to implement and with low computational complexities. However, the results from these metrics are in close agreement with human judgments. These results gives further credence to lack of consistency with subjective human evaluation associated with MSE and PSNR. The experimental results clearly show that the combination of power spectra and SSIM would prove more effective and efficient in image quality assessment. It work accurately and can measure quality across distortion types when compared with MSE and PSNR. The simulated results for power spectrum showed that the better the quality of the image the clearer and understandable the frequency spectrum.

6.0 References

[1] Fierrez-Aguilar, J., Chen, Y., Ortega-Garcia, J. and Jain, A.K., 2006, January. Incorporating image quality in multi-algorithm fingerprint verification. In International Conference on Biometrics (pp. 213-220). Springer Berlin Heidelberg.

[2] Li, C., Bovik, A.C. and Wu, X., 2011. Blind image quality assessment using a general regression neural network. IEEE Transactions on Neural Networks, 22(5), pp.793-799.

[3] Moorthy, A.K., Su, C.C., Mittal, A. and Bovik, A.C., 2013. Subjective evaluation of stereoscopic image quality. Signal Processing: Image Communication, 28(8), pp.870-883.

[4] Wang, Z., Bovik, A.C., Sheikh, H.R. and Simoncelli, E.P., 2004. Image quality assessment: from error visibility to structural similarity. IEEE transactions on image processing, 13(4), pp.600-612.

[5] Chandrakanth, T. and Sandhya, B., 2016. Analysis of SSIM based Quality Assessment across Color Channels of Images. In Human-Computer Interaction: Concepts, Methodologies, Tools, and Applications (pp. 1233-1245). IGI Global.

[6] ECE, C. and Mullana, M.M.U., 2011. Image quality assessment techniques pn spatial domain. Int. J. Comput. Sci. Technol, 2(3).

[7] Shermina, J. and Vasudevan, V., 2011. An efficient face recognition system based on the hybridization of invariant pose and illumination process. European Journal of Scientific Research, 64(2), pp.225-243.

[8] Abate, A.F., Nappi, M., Riccio, D. and Sabatino, G., 2007. 2D and 3D face recognition: A survey. Pattern recognition letters, 28(14), pp.1885-1906.

[8] Zhuang, L., Yang, A.Y., Zhou, Z., Shankar Sastry, S. and Ma, Y., 2013. Single-sample face recognition with image corruption and misalignment via sparse illumination transfer. In Proceedings of the IEEE Conference on Computer Vision and Pattern Recognition (pp. 3546-3553).

[9] Kumar, P. and Shibu, S., 2014. Authorization of Face Recognition Technique Based on Eigen Faces. International Journal of Advanced Research in Computer and Communication Engineering, 3(9).

[10] DiCarlo, J.M., Xiao, F. and Wandell, B.A., 2001, January. Illuminating illumination. In Color and Imaging Conference (Vol. 2001, No. 1, pp. 27-34). Society for Imaging Science and Technology.

[11] Kukula, E.P. and Elliott, S.J., 2004. Evaluation of a facial recognition algorithm across three illumination conditions. IEEE Aerospace and Electronic Systems Magazine, 19(9), pp.19-23.

[12] Jiang, D., Hu, Y., Yan, S., Zhang, L., Zhang, H. and Gao, W., 2005. Efficient 3D reconstruction for face recognition. Pattern Recognition,38(6), pp.787-798.

[13] Arandjelović, O. and Cipolla, R., 2013. Damera-Venkata, N., Kite, T.D., Geisler, W.S., Evans, B.L. and Bovik, A.C., 2000. Image quality assessment based on a degradation model.IEEE transactions on image processing, 9(4), pp.636-650. Pattern Recognition, 46(1), pp.9-23.

[14] Romdhani, S., Ho, J., Vetter, T. and Kriegman, D.J., 2006. Face recognition using 3-D models: Pose and illumination. Proceedings of the IEEE, 94(11), pp.1977-1999.

[15] Damera-Venkata, N., Kite, T.D., Geisler, W.S., Evans, B.L. and Bovik, A.C., 2000. Image quality assessment based on a degradation model.IEEE transactions on image processing, 9(4), pp.636-650.

[16] Li, Q., Yin, W. and Deng, Z., 2010. Image-based face illumination transferring using logarithmic total variation models. The visual computer,26(1), pp.41-49.

[17] Anbarjafari, G., Jafari, A., Jahromi, M.N.S., Ozcinar, C. and Demirel, H., 2015. Image illumination enhancement with an objective no-reference measure of illumination assessment based on Gaussian distribution mapping. Engineering Science and Technology, an International Journal,18(4), pp.696-703.

[18] Ho, J. and Kriegman, D., 2005. On the effect of illumination and face recognition. Face Processing: Advanced Modeling and Methods.

[19] De Carrera, P.F. and Marques, I., 2010. Face recognition algorithms.Master's thesis in Computer Science, Universidad Euskal Herriko.

[20] Zhao, W. and Chellappa, R., 2002. Image-based face recognition: Issues and methods. OPTICAL ENGINEERING-NEW YORK-MARCEL DEKKER INCORPORATED-, 78, pp.375-402.

[21] Polder, G., Van der Heijden, G.W.A.M. and Young, I.T., 2002. Spectral image analysis for measuring ripeness of tomatoes. Transactions-American Society of Agricultural Engineers, 45(4), pp.1155-1162.

[22] Senthil, K., Karunanithi, N., Kim, G.S., Nagappan, A., Sundareswaran, S., Natesan, S. and Muthurajan, R., 2011. Proteome analysis of in vitro and in vivo root tissue of Withania somnifera. African Journal of Biotechnology,10(74), pp.16866-16874.

[23] Hu, Y. and Loizou, P.C., 2008. Evaluation of objective quality measures for speech enhancement. IEEE Transactions on audio, speech, and language processing, 16(1), pp.229-238.

[24] Lee, J. and Park, R.H., 2015. Image Quality Assessment of Tone Mapped Images. International Journal of Computer Graphics & Animation, 5(2), p.9.

[25] Wang, Z., Li, L., Wu, S., Xia, Y., Wan, Z. and Cai, C., 2015. A New Image Quality Assessment Algorithm based on SSIM and Multiple Regressions.International Journal of Signal Processing, Image Processing and Pattern Recognition, 8(11), pp.221-230.

[26] Raijada, M.K., Patel, M.D. and Prajapati, M.P., 2015, February. A Review Paper on Image Quality Assessment Metrics. In Journal of Emerging Technologies and Innovative Research (Vol. 2, No. 1 (February-2015)). JETIR.

[27] Battisti, F., Bosc, E., Carli, M., Le Callet, P. and Perugia, S., 2015. Objective image quality assessment of 3D synthesized views. Signal Processing: Image Communication, 30, pp.78-88.

[28] Mittal, A., Moorthy, A.K. and Bovik, A.C., 2012. No-reference image quality assessment in the spatial domain. IEEE Transactions on Image Processing, 21(12), pp.4695-4708.

[29] Gundimada, S. and Asari, V., 2004, April. Face detection technique based on rotation invariant wavelet features. In Information Technology: Coding and Computing, 2004. Proceedings. ITCC 2004. International Conference on (Vol. 2, pp. 157-158). IEEE.

[30] Wang, Z. and Simoncelli, E.P., 2005, March. Reduced-reference image quality assessment using a wavelet-domain natural image statistic model. In Electronic Imaging 2005 (pp. 149-159). International Society for Optics and Photonics.

[31] Zhang, F., Ma, L., Li, S. and Ngan, K.N., 2011. Practical image quality metric applied to image coding. IEEE Transactions on Multimedia, 13(4), pp.615-624.

[32] Larson, E.C. and Chandler, D.M., 2010. Most apparent distortion: full-reference image quality assessment and the role of strategy. Journal of Electronic Imaging, 19(1), pp.011006-011006.

[33] Liang, L., Wang, S., Chen, J., Ma, S., Zhao, D. and Gao, W., 2010. No-reference perceptual image quality metric using gradient profiles for JPEG2000. Signal Processing: Image Communication, 25(7), pp.502-516.

[34] Zhang, L., Zhang, L., Mou, X. and Zhang, D., 2011. FSIM: A feature similarity index for image quality assessment. IEEE transactions on Image Processing, 20(8), pp.2378-2386.

[35] Wang, Z., Simoncelli, E.P. and Bovik, A.C., 2003, November. Multiscale structural similarity for image quality assessment. In Signals, Systems and Computers, 2004. Conference Record of the Thirty-Seventh Asilomar Conference on (Vol. 2, pp. 1398-1402). IEEE.

[36] Nikvand, N. and Wang, Z., 2013. Image distortion analysis based on normalized perceptual information distance. Signal, Image and Video Processing, 7(3), pp.403-410.

[37] Hore, A. and Ziou, D., 2010, August. Image quality metrics: PSNR vs. SSIM. In Pattern Recognition (ICPR), 2010 20th International Conference on (pp. 2366-2369). IEEE.

[38] Rippel, O., Snoek, J. and Adams, R.P., 2015. Spectral representations for convolutional neural networks. In Advances in Neural Information Processing Systems (pp. 2449-2457).

[39] De Silva, V., Arachchi, H.K., Ekmekcioglu, E. and Kondoz, A., 2013. Toward an impairment metric for stereoscopic video: A full-reference video quality metric to assess compressed stereoscopic video. IEEE transactions on image processing, 22(9), pp.3392-3404.

[40] Ma, K., Zhao, T., Zeng, K. and Wang, Z., 2015. Objective quality assessment for color-to-gray image conversion. IEEE Transactions on Image Processing, 24(12), pp.4673-4685.

[41] Tong, Y., Konik, H., Cheikh, F. and Tremeau, A., 2010. Full reference image quality assessment based on saliency map analysis. Journal of Imaging Science and Technology, 54(3), pp.30503-1.

[42] Ebrahimi Moghadam, A., Mohammadi, P. and Shirani, S., 2015. Subjective and Objective Quality Assessment of Image: A Survey. Majlesi Journal of Electrcial Engineering, 9.

[43] Lin, Y.H. and Wu, J.L., 2014. Quality assessment of stereoscopic 3D image compression by binocular integration behaviors. IEEE transactions on Image Processing, 23(4), pp.1527-1542.

[44] Yeganeh, H. and Wang, Z., 2013. Objective quality assessment of tone-mapped images. IEEE Transactions on Image Processing, 22(2), pp.657-667.

[45] Narwaria, M. and Lin, W., 2010. Objective image quality assessment based on support vector regression. IEEE Transactions on Neural Networks, 21(3), pp.515-519.

[46] Quackenbush, S.R., Barnwell, T.P. and Clements, M.A., 1988. Objective measures of speech quality. Prentice Hall.

[47] Campanella, G., Pereira, A., Ribeiro, R.A. and Varela, M.L.R., 2011, June. Collaborative dynamic decision making: A case study from B2B supplier selection. In Euro Working Group Workshop on Decision Support Systems (pp. 88-102). Springer Berlin Heidelberg.

[48] Chan, C.C.H., Cheng, C.B. and Hsu, C.H., 2008. Bargaining strategy formulation with CRM for an e-commerce agent. Electronic Commerce Research and Applications, 6(4), pp.490-498.

[49] Rehman, A. and Wang, Z., 2012. Reduced-reference image quality assessment by structural similarity estimation. IEEE Transactions on Image Processing, 21(8), pp.3378-3389.

[50] Sheikh, H.R., Bovik, A.C. and Cormack, L., 2005. No-reference quality assessment using natural scene statistics: JPEG2000. IEEE Transactions on Image Processing, 14(11), pp.1918-1927.

[51] Fang, Y., Qureshi, I., Sun, H., McCole, P., Ramsey, E. and Lim, K.H., 2014. Trust, Satisfaction, and Online Repurchase Intention: The Moderating Role of Perceived Effectiveness of E-Commerce Institutional Mechanisms.Mis Quarterly, 38(2), pp.407-427.

[52] Al-Obaidi, F.E., 2015. Image Quality Assessment for Defocused Blur Images. American Journal of Signal Processing, 5(3), pp.51-55.

[53] Okarma, K., 2008, November. Colour image quality assessment using structural similarity index and singular value decomposition. InInternational Conference on Computer Vision and Graphics (pp. 55-65). Springer Berlin Heidelberg.

[54] Kusuma, T.M. and Zepernick, H.J., 2003, October. A reduced-reference perceptual quality metric for in-service image quality assessment. InMobile Future and Symposium on Trends in Communications, 2003. SympoTIC'03. Joint First Workshop on (pp. 71-74). IEEE.

[55] Bensalma, R. and Larabi, M.C., 2013. A perceptual metric for stereoscopic image quality assessment based on the binocular energy.Multidimensional Systems and Signal Processing, 24(2), pp.281-316.

[56] Chandler, D.M., 2013. Seven challenges in image quality assessment: past, present, and future research. ISRN Signal Processing, 2013.

[57] Russo, I., Confente, I., Gligor, D.M. and Autry, C.W., 2016. To be or not to be (loyal): Is there a recipe for customer loyalty in the B2B context?.Journal of Business Research, 69(2), pp.888-896.

[58] Brandão, T. and Queluz, M.P., 2008. No-reference image quality assessment based on DCT domain statistics. Signal Processing, 88(4), pp.822-833.

[59] Chen, M.J., Cormack, L.K. and Bovik, A.C., 2013. No-reference quality assessment of natural stereopairs. IEEE Transactions on Image Processing, 22(9), pp.3379-3391.

[60] Shahid, M., Rossholm, A., Lövström, B. and Zepernick, H.J., 2014. No-reference image and video quality assessment: a classification and review of recent approaches. EURASIP Journal on image and Video Processing,2014(1), p.40.

[61] Ferzli, R. and Karam, L.J., 2009. A no-reference objective image sharpness metric based on the notion of just noticeable blur (JNB). IEEE transactions on image processing, 18(4), pp.717-728.

[62] Hassen, R., Wang, Z. and Salama, M.M., 2013. Image sharpness assessment based on local phase coherence. IEEE Transactions on Image Processing, 22(7), pp.2798-2810.

[63] Sheikh, H.R. and Bovik, A.C., 2006. Image information and visual quality.IEEE Transactions on image processing, 15(2), pp.430-444.

[64] Balboa, R.M. and Grzywacz, N.M., 2003. Power spectra and distribution of contrasts of natural images from different habitats. Vision research,43(24), pp.2527-2537.

[65] Van der Schaaf, V.A. and van Hateren, J.V., 1996. Modelling the power spectra of natural images: statistics and information. Vision research,36(17), pp.2759-2770.

[66] Larson, D., Dunkley, J., Hinshaw, G., Komatsu, E., Nolta, M.R., Bennett, C.L., Gold, B., Halpern, M., Hill, R.S., Jarosik, N. and Kogut, A., 2011. Seven-year wilkinson microwave anisotropy probe (WMAP*) observations: power spectra and WMAP-derived parameters. The Astrophysical Journal Supplement Series, 192(2), p.16.

[67] Gavrila, R., Dinescu, A. and Mardare, D., 2007. A power spectral density study of thin films morphology based on AFM profiling. Raman J Inf Sci Technol, 10, pp.291-300.

[68] van Lare, M.C. and Polman, A., 2015. Optimized scattering power spectral density of photovoltaic light-trapping patterns. ACS Photonics, 2(7), pp.822-831.

[69] Torralba, A. and Oliva, A., 2003. Statistics of natural image categories.Network: computation in neural systems, 14(3), pp.391-412.

[70] Channappayya, S.S., Bovik, A.C., Caramanis, C. and Heath, R.W., 2008, March. SSIM-optimal linear image restoration. In Acoustics, Speech and Signal Processing, 2008. ICASSP 2008. IEEE International Conference on(pp. 765-768). IEEE.

[71] Narwaria, M., Lin, W. and Cetin, A.E., 2012. Scalable image quality assessment with 2D mel-cepstrum and machine learning approach.Pattern Recognition, 45(1), pp.299-313.

[72] McAndrew, A., 2004. An introduction to digital image processing with matlab notes for scm2511 image processing. School of Computer Science and Mathematics, Victoria University of Technology, pp.1-264.

[73] Lewis, A.S. and Knowles, G., 1992. Image compression using the 2-D wavelet transform. IEEE transactions on image processing, 1(2), pp.244-250